Independent Confirmation of Global Land Warming without the Use of Land Thermometers

Gilbert P. Compo[1,2], Prashant D. Sardeshmukh[1,2], Jeffrey S. Whitaker[2], Philip Brohan[3], Philip D. Jones[4], Chesley McColl[1,2]

1) Climate Diagnostics Center, CIRES, University of Colorado, Boulder, CO, USA
2) Physical Sciences Division, Earth System Research Laboratory, NOAA, Boulder, CO, USA
3) Met Office Hadley Centre, Exeter, UK
4) Climatic Research Unit, University of East Anglia, Norwich, UK

Confidence in estimates of anthropogenic climate change is limited by known difficulties with air temperature observations from land stations. We test those observations using a completely different approach to investigate global land warming over the 20th century. We have ignored all of the land temperature observations and instead inferred the temperature from observations of the barometric pressure and the sea surface temperature and sea-ice concentration using a physically-based data assimilation system called the 20th Century Reanalysis (20CR). This independent dataset *reproduces both annual variations and centennial trends in the observation-based near-surface land air temperature datasets*.

Summary

1) Site moves, instrument changes, changing observing practices, urban effects, land use variations, and statistical processing have debatable effects on the trends[1,2,3] presented by the Intergovernmental Panel on Climate Change[4] and others[5-9].

2) Deduce the global land warming **without using any of the land temperature observations** by instead using the 20th Century Reanalysis[10] (20CR), a physically-based, state-of-the-art data assimilation system, to infer land temperatures from monthly-averaged sea surface temperature (SST) and sea ice concentration[11], and from subdaily barometric pressure observations around the globe. ***Time variation of 20CR (Fig. 1) and spatial pattern of trends (Fig. 2) are very similar to those previously reported (Table 1).***

3) Also use an ensemble of AGCM integrations; with same prescribed SST, sea-ice, radiative forcings, and model as in 20CR but without using any pressure observations. Though the SSTs are expected to be the dominant contributor to land warming, both regionally[13] and globally[13,14], 20CR corresponds better to the station datasets than it does to the AGCM ensemble (Table 1, Fig. 2), particularly on the monthly timescale (Table 1), confirming the important influence of the pressure observations.

Global land average (90°N-60°S) annual anomaly time series compare well between pressure-based reanalysis 20CR and station temperature datasets.

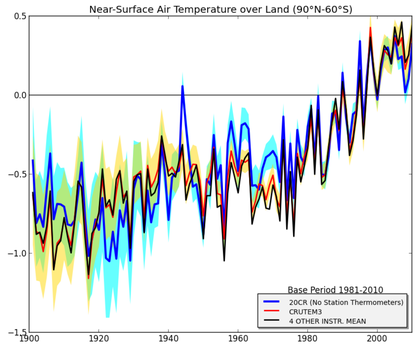

Figure 1. Global land (90°N-60°S) 2 m air temperature from 20CR[10] and instrumental estimates. (Red curve) global temperature anomaly series from the CRUTEM3 thermometer-based dataset[5], (black curve) the average of four additional thermometer-based datasets (* in Table 1), and (blue curve) the pressure-based 20CR. 95% uncertainty ranges are shown for CRUTEM3 (yellow fill) and 20CR (blue fill) and their overlap (green fill).

The correlation between 20CR and CRUTEM3 is 0.91.

Patterns and magnitude of the multi-decadal trends are similar between 20CR and the station-based datasets. Some regional differences are present.

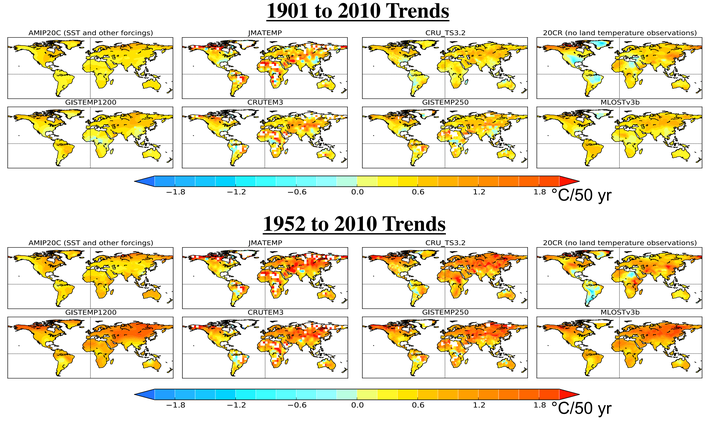

Figure 2. Comparison of local linear trends of global land (90°N-60°S) 2 m air temperature between 20CR[10], station-temperature based estimates, and AGCM SST-forced simulation (AMIP20C). Trends shown as °C change per 50 years over the (top) 1901-2010 and (bottom) 1952-2010 periods.

Pattern correlations between 20CR and other dataset trends range from (1901-2010) 0.67 to 0.76 and (1952-2010) 0.73 to 0.81. The more rapid warming of the 1952-2010 period is captured (Table 1).

Global land temperature anomalies from 20CR over the periods 1901 to 2010 and 1952 to 2010 are quantitatively similar to station-temperature estimates.

Table 1. Global land temperature anomalies (90°N-60°S) from 20CR[10] over the periods 1901 to 2010 and 1952 to 2010 compared with station-temperature estimates and an AGCM simulation using the same 56 member ensemble, SSTs, radiative forcings, and numerical model configuration as 20CR but with no data assimilation (AMIP20C). 1952 marks the starting year in which 20CR uncertainty parameterizations representing model error and sampling error remain constant[10]. 90°N-60°S is the region common to all data sets considered. * indicates data sets used in the four dataset average of Fig. 1. *Temporal Correlation Annual* shows the correlation coefficient between the 20CR and observed and simulated globally-averaged annual anomaly temperature series. All p-values are 0.99 or larger. *Temporal Correlation Monthly High Pass* shows the correlation coefficient between the 20CR and observed and simulated globally-averaged monthly anomalies after a 7-year running mean has been removed from each series. All p-values are 0.999 or larger. Temporal significance tests account for the reduction in temporal degrees of freedom (dof) arising from the auto-correlation in all series[15]. *Pattern Correlation* shows the area-weighted pattern correlation[16] between the 20CR and observed and simulated temperature trend fields. All p-values are greater than 0.965 assuming 8 spatial dof. The pattern correlation with the area-mean removed is shown with parentheses. The *Percentage Larger* is the areal coverage of station-temperature or simulated local temperature changes that are larger than 20CR. None of these percentages are statistically distinguishable from the 50% expected for a binomial distribution if the dof of the temperature trend field are less than 22. Estimates of the dof range from 3 to 8[17]. *Trend* is the area-weighted globally-averaged linear trend for each data set computed as the average of the local linear trends. 20CR land-average trend is 0.45 K/50 years (1901-2010) and 0.67 K/50 years (1952-2010). None of these reported trends are significantly different from 20CR trends assuming 8 spatial dof (all p-values are 0.855 or less).

	Temporal Correlation Annual	*Temporal Correlation Monthly High Pass*	*Pattern correlation (area mean removed)*	*Percentage Larger*	*Trend (change in °C per 50 years)*
1901-2010					
CRUTEM3*	0.91	0.76	0.70 (0.23)	60%	0.55
CRU_TS3.2*,+	0.90	0.81	0.72 (0.33)	47%	0.42
GISTEMP250*,+	0.88	0.78	0.67 (0.22)	56%	0.50
GISTEMP1200*	0.85	0.87	0.72 (0.26)	47%	0.43
JMATEMP*,+	0.89	0.74	0.67 (0.27)	63%	0.68
MLOST*,+	0.90	0.81	0.76 (0.34)	54%	0.48
AMIP20C	0.89	0.35	0.74 (0.28)	48%	0.45
1952-2010					
CRUTEM3*	0.95	0.84	0.78 (0.39)	71%	0.87
CRU_TS3.2*,+	0.96	0.86	0.77 (0.37)	69%	0.96
GISTEMP250*,+	0.96	0.85	0.73 (0.31)	71%	0.88
GISTEMP1200*	0.96	0.85	0.81 (0.44)	73%	0.98
JMATEMP*,+	0.95	0.82	0.76 (0.36)	68%	1.0
MLOST*,+	0.96	0.86	0.80 (0.39)	73%	0.96
AMIP20C	0.89	0.36	0.73 (0.15)	52%	0.65

References

1) Pielke, R. A., Sr., et al., Unresolved issues with the assessment of multidecadal global land surface temperature trends, J. Geophys. Res., 112, D24S08 (2007).
2) Klotzbach, P. J., et al., An alternative explanation for differential temperature trends at the surface and in the lower troposphere, J. Geophys. Res., 114, D21102 (2009).
3) Parker, D. E., Recent land surface air temperature trends assessed using the 20th Century Reanalysis, J. Geophys. Res., 116, D20125 (2011).
4) Trenberth, K.E., et al., Observations: Surface and Atmospheric Climate Change. In: Climate Change 2007: The Physical Science Basis. Contribution of Working Group 1 to the Fourth Assessment Report of IPCC [Solomon, S., et al. (eds.)], pp235-336, Cambridge University Press, Cambridge, United Kingdom and New York, NY, USA (2007).
5) Brohan P, et al., Uncertainty estimates in regional and global observed temperature changes: A new data set from 1850. J Geophys Res 111:D12106 (2006).
6) Hansen, J., et al., Global surface temperature change, Rev. Geophys., 48, RG4004 (2010).
7) Ishii, M., et al. (2005), Objective analyses of sea-surface temperature and marine meteorological variables for the 20th century using ICOADS and the Kobe collection, Int. J. Climatol., 25, 865–879 (2005).
8) Japan Meteorological Agency, Global surface temperature anomalies data, available at http://ds.data.jma.go.jp/tcc/tcc/products/gwp/gwp.html (2011).
9) Smith TM, Reynolds RW, A global merged land-air-sea surface temperature reconstruction based on historical observations (1880-1997). J Clim 18:2021-2036 (2005).
10) Compo, G.P., et al., The Twentieth Century Reanalysis Project. Quarterly J. Roy. Meteorol. Soc., 137, 1-28 (2011).
11) Rayner NA, et al (2003) Global analyses of sea surface temperature, sea ice, and night marine air temperatures since the late nineteenth century. J. Geophys. Res.,108 (D14): 4407 (2003).
12) Mitchell and P.D. Jones, An improved method of constructing a database of monthly climate observations and associated high-resolution grids. Int. J. Climatology, 25, 693-712, (2005).
13) Compo, G.P., P.D. Sardeshmukh, Oceanic influences on recent continental warming. Climate Dynamics, 32, 333-342 (2009).
14) Hoerling, M., et al. (2008), What is causing the variability in global mean land temperature?, *Geophys. Res. Lett.*, 35, L23712 (2008).
15) Livezey R.E., W.Y. Chen, Statistical Field Significance and its Determination by Monte Carlo Techniques, Mon. Wea. Rev., 111, 46-59 (1983).
16) Miyakoda K, Hembree GD, Strickler RF, Shulman I, Cumulative results of extended forecast experiments I: Model performance for winter cases. Mon. Wea. Rev. 100: 836-855 (1972).
17) Jones PD, Osborn TJ, Briffa KR, Estimating sampling errors in large-scale temperature averages. J Clim 10:2548-2568 (1997).